

CrystEngComm

Accepted Manuscript



This is an *Accepted Manuscript*, which has been through the Royal Society of Chemistry peer review process and has been accepted for publication.

Accepted Manuscripts are published online shortly after acceptance, before technical editing, formatting and proof reading. Using this free service, authors can make their results available to the community, in citable form, before we publish the edited article. We will replace this *Accepted Manuscript* with the edited and formatted *Advance Article* as soon as it is available.

You can find more information about *Accepted Manuscripts* in the [Information for Authors](#).

Please note that technical editing may introduce minor changes to the text and/or graphics, which may alter content. The journal's standard [Terms & Conditions](#) and the [Ethical guidelines](#) still apply. In no event shall the Royal Society of Chemistry be held responsible for any errors or omissions in this *Accepted Manuscript* or any consequences arising from the use of any information it contains.

Calcium Carbonate Crystallization in Tailored Constrained Environments

C. Beato^a, M. S. Fernández^a, S. Fermani^b, M. Reggi^b, A. Neira-Carrillo^a, A. Rao^c, G. Falini^b, and
J. L. Arias^a

Abstract

The synthesis of inorganic particles using routes inspired by biomineralization is a goal of growing interest. Recently it was demonstrated that the size and geometry of the crystallization site are as important as the structure of the charged templating surfaces to obtain particles with controlled features. Most biominerals are formed inside restricted, constrained or confined spaces where at least part of the boundaries, are cell membranes containing phospholipids. In this study, we used a gas diffusion method to determine the effect of different lecithin media on the crystallization of CaCO₃ and to evaluate the influence of the spatial arrangement of lecithin molecules on templating CaCO₃ crystal formation. By using inorganic synthesis, Raman spectroscopy, dynamic light scattering, electrochemical methods and scanning electron microscopy, we showed that the occurrence of surface-modified calcite crystals and diverse textured vaterite crystals reflects the geometry and spatial distribution of aqueous constrained spaces due to the lecithin assembly controlled by lecithin concentration in an ionized calcium chloride solution under a continuous CO₂ diffusion atmosphere. This research shows that by tailoring the assembly of lecithin molecules, as micelle or reversed micelle, it is possible to modulate texture, polymorphism, size and shape of calcium carbonate crystals.

^a*Faculty of Veterinary Sciences, University of Chile, Santiago, Chile. E-mail: jarias@uchile.cl*

^b*Department of Chemistry "Giacomo Ciamician," Alma Mater Studiorum University of Bologna, Italy.*

^c*Department of Chemistry, University of Konstanz, Constance, Germany.*

Introduction

Biom mineralization refers to the process by which organisms precipitate inorganic minerals on an organic template.¹⁻³ Biom minerals present unique morphologies and hierarchical structures which strongly determines their functions and mechanical properties. Several studies have demonstrated that organic templates, such as proteins, carbohydrates or synthetic polymers, are able to control inorganic crystal growth.⁴⁻¹⁰ Complementarity to the inorganic phase surface structure, charge and geometrical configuration, and binding energies are important aspects of this influence.^{11, 12} Most biom minerals are formed inside confined spaces where at least part of the boundaries are cell membranes containing phospholipids. Among known biom minerals, calcium carbonate (CaCO_3) is one of the most studied minerals and presents different structural forms referred to as calcite, aragonite, vaterite, monohydrocalcite, hexahydrocalcite and amorphous calcium carbonates (ACC).¹³ The occurrence of these forms depends on the kinetics and thermodynamics of the reaction of CaCO_3 formation,¹⁴ which is particularly influenced by the interaction of the mineral with the organic moiety.¹⁵ To study the effect of confinement on biom mineralization, different model systems have been developed focusing on the precipitation of ACC. Several groups have reported an increased lifetime for ACC when confined in pores,¹⁶ between crossed cylinders,¹⁷ in picoliter droplets,¹⁸ within a silica coating,¹⁹ or in liposomes.²⁰ Other studies using confined aqueous nano- or picovolume droplets in oil have shown that precipitation of CaCO_3 occurs via hydrated forms instead of ACC.²¹ However, in porous media such as gel systems, which are not completely confined, pore size strongly influences nucleation.²²

In biological systems, most likely a combination of all of these phenomena occurs in such a way that a comparative analysis of a variety of biomineralized systems has led to the following general principles:^{2, 23}

1. Biomineralization occurs within specific confined microenvironments, which implies crystal production at certain functional sites and inhibition or prevention of the process at other sites.
2. A specific mineral is produced with a defined crystal size and orientation.
3. Macroscopic growth is accomplished by packing many incremental units together; this results in unique composites with layered microarchitectures that impart peculiar properties.

Main compartments in biology are cells, tissues or extracellular matrix, meaning that confinement for mineral formation occurs in an environment which is partly surrounded by cellular membranes, that is, lipid bilayers.

Phospholipids like dipalmitoylphosphatidylcholine (DPPC), commonly known as lecithin, are principal components of the cell membrane. The polar part of the lecithin molecule has two spatially separated and oppositely charged moieties: the positive choline group and the negative phosphate group.²⁴ In an aqueous medium, lecithin molecules form micelles, wherein the hydrophobic groups are arranged inward while the hydrophilic groups are arranged outwards. In previous studies it has been found that when the soluble medium contains calcium ions (Ca^{+2}), an interaction occurs between the ions and the surface of the lipid vesicles. This is the basis for intermicellar CaCO_3 crystallization.²⁵

Although there are several studies regarding the effect of phospholipid molecules on the *in vitro* biomineralization process^{42, 26-31}, there has been no analysis of the effect of micelle spatial arrangement on the crystallization of CaCO_3 . In this study we used a gas diffusion method to

determine the effect of different lecithin media on the crystallization of CaCO_3 and to evaluate the influence of the spatial arrangement of lecithin molecules on templating CaCO_3 crystal formation.

Experimental

To determine the effect of lecithin on CaCO_3 crystal formation, a gas diffusion method was used (Fig. 1).^{32, 33}

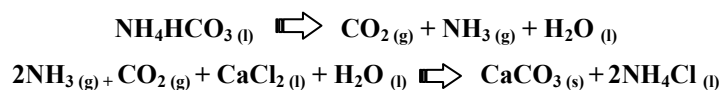
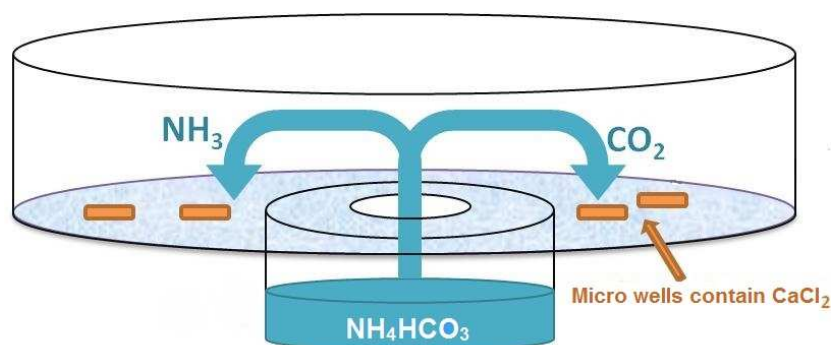


Fig. 1. Experimental chamber. Ammonium bicarbonate (NH_4HCO_3) placed in the cylindrical container decomposes into ammonia (NH_3) and carbon dioxide (CO_2), forming an atmosphere of CO_2 and NH_3 . These gasses diffuse into the calcium chloride (CaCl_2) solution producing conditions for formation of calcium carbonate (CaCO_3) in the micro wells.

Briefly, it consists of a Petri dish of 85 mm diameter with a 10-mm hole in its base to allow communication with a cylindrical glass vessel of 50 mm diameter and 30 mm height that is attached to the Petri dish (Fig. 1). The base plate was divided into ten equal circular sectors,

where polystyrene micro wells (microbridges; Hampton Res, Aliso Viejo, CA) were placed. In each micro well 35 μl of 200 mM CaCl_2 in TRIS buffer, pH 9, with or without lecithin at different concentrations were added.

Four lecithin stock solutions were prepared at concentrations of 1.6 mg/ml, 10 mg/ml, 150 mg/ml and 300 mg/ml. All solutions were prepared with lecithin Vital Nature®, which was dissolved in deionized water. To obtain a homogeneous emulsion, the solutions were sonicated with a Branson Digital Sonifier (Merck) for 20 minutes in continuous mode at 10% amplitude. Sonication was done ice to avoid an increase of solution temperature. Different mass ratios of CaCl_2 /lecithin solutions were added to the micro wells as described in Table 1.

Dynamic light scattering was used for determination of the lecithin particle size distributions employing a Malvern Nano ZS instrument with a 633 nm laser diode. Experiments were carried out at 25 °C in a quartz cuvette of 1 cm optical path length. The conductivity was measured with a conductometric cell (Metrohm No. 6.0910.120) connected via a conductivity module (856, Metrohm No. 2.856.0010) to a computer. For crystal formation, 3 ml of NH_4HCO_3 solution were placed in the cylindrical vessel, and the Petri dish was covered with a glass lid, sealed with Parafilm® and allowed to stand for 24 hours at room temperature. Then the micro wells were washed 2 times with distilled water, then with 50%, 80% and 100% ethanol solutions, and finally 2 washes with 5% sodium hypochlorite solution. The washes with 5% sodium hypochlorite were necessary to observe crystals in the conditions where lecithin formed a highly viscous sol. The 5% sodium hypochlorite solution acted as an oxidizing agent to remove the lecithin and did not affect the shape and morphology of the crystals already formed.

A DeltaNu Advantage Systems Raman spectrometer was used to obtain the Raman spectra of the precipitates that formed. Analysis of the Raman spectra of the precipitates was done to determine the polymorphism of the crystals that formed.

Micro wells were coated with gold by using electron microscopy science EMS-550 equipment (Automated Sputter Coated). Micro wells were observed by scanning electron microscopy (SEM) with a Tesla BS-343A instrument using 15 kV and with a FEG SEM Hitachi 6400 instrument. The average crystal size was obtained by measuring crystals from four pictures of different fields. The values were statistically analyzed by R Studio program to obtain the mean values and standard deviation for each population of crystals.

Table 1. Micro well codes of lecithin quantity (μg) in 35 μL of TRIS/ CaCl_2 solution. The hydrodynamic radius of lecithin particles determined by a measure of dynamic light scattering is also reported: the standard error is indicated.

MICRO WELL CODE	LECITHIN SOLUTION ADDED TO 100 μl OF 0.2 M CaCl_2	LECITHIN QUANTITY IN THE MICRO WELL ($\mu\text{g}/35 \mu\text{L}$ of solution)	HYDRODYNAMIC RADIUS (nm)
M0	0	0	-
M1	1 μl of 1.6 mg/ml	0.56	88.9 \pm 4.9
M2	5 μl of 1.6 mg/ml	2.8	98.3 \pm 2.7
M3	10 μl of 1.6 mg/ml	5.6	104.0 \pm 4.3
M4	1 μl of 10 mg/ml	3.5	91.8 \pm 8.9
M5	5 μl of 10 mg/ml	17.5	125.0 \pm 2.6
M6	10 μl of 10 mg/ml	35	124.1 \pm 7.6
M7	1 μl of 150 mg/ml	52.5	n.d.*
M8	5 μl of 150 mg/ml	262.5	n.d.
M9	10 μl of 150 mg/ml	525	n.d.
M10	1 μl of 300 mg/ml	105	n.d.
M11	5 μl of 300 mg/ml	525	n.d.
M12	10 μl of 300 mg/ml	1050	n.d.

*n.d. not determined

Results

The aggregation of lecithin in the 200 mM CaCl₂ solution was analyzed by dynamic light scattering. In the stock solutions obtained by dissolution of lecithin in water, the hydrodynamic radii of lecithin aggregates were 29.1±5.6 nm, 22.4±2.3 nm, 23.7±4.1 nm and 20.0±3.6 nm at a concentration of 1.6 mg/ml, 10 mg/ml, 150 mg/ml and 300 mg/ml, respectively. When different aliquots of a lecithin stock solution were diluted in 100 ml of 200 mM CaCl₂ solution a large increase was observed in the hydrodynamic radius of the lecithin particles. The translucent liquid solutions obtained in the less concentrated lecithin samples were increasingly transformed into more opaque highly viscous sols when lecithin concentration was increased. Therefore, the hydrodynamic radius was around 100 nm when low concentrations of lecithin were used, and the radius was not determined in the more highly concentrated viscous sols. Conductivities for 1.6 mg/ml and 300 mg/ml lecithin in Milli-Q water were 0.099±0.02 mS/cm and 0.57±0.06 mS/cm, respectively. However, in 200 mM CaCl₂ in pH 9 TRIS buffer, the conductivity for 1.6 mg/ml lecithin was 27 mS/cm, while the conductivity for 300 mg/ml lecithin was 7.7 mS/cm. After 24 h on the bench, the conductivity decreased to 20.3 mS/cm and 6.6 mS/cm, respectively.

To determine the CaCO₃ polymorphism, Raman spectra were analyzed by comparison with calcite, aragonite and vaterite standard spectra reported by Wehrmeister *et al.*³² Raman spectra were measured in the micro wells without any solution or glass, and Raman spectra for M0 and M10 micro wells are shown in Fig. 2.

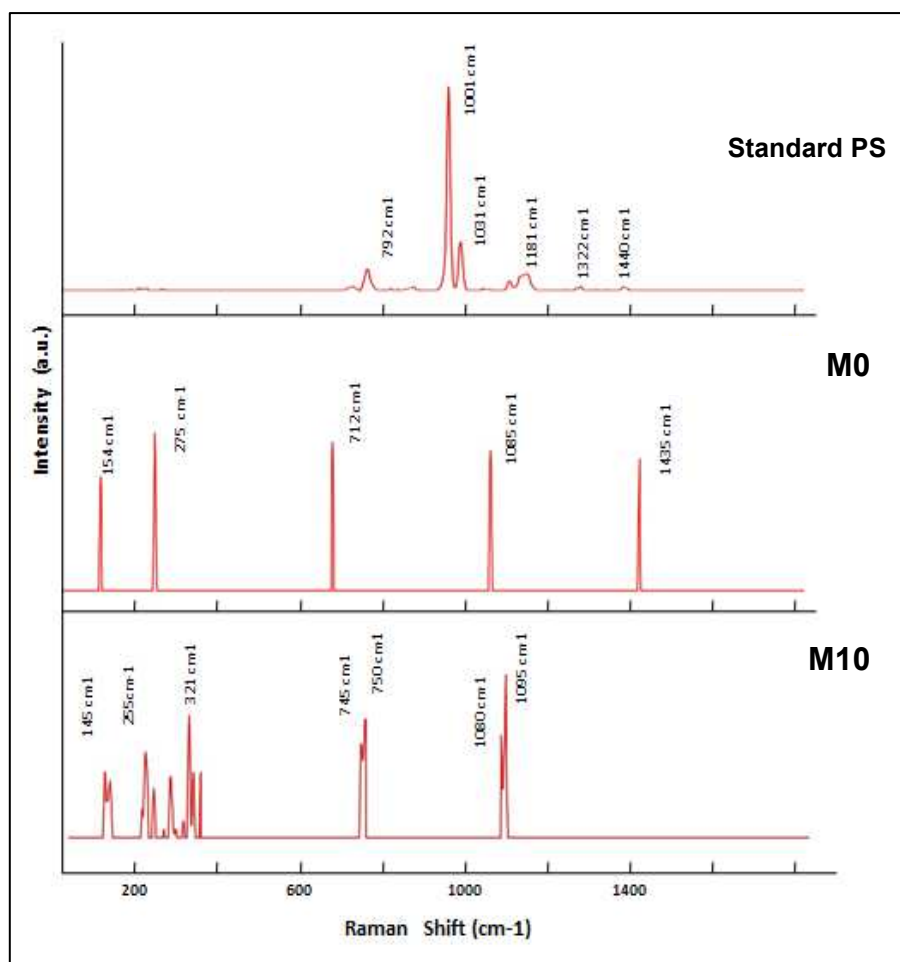


Fig. 2. M0 and M10 polystyrene micro well Raman spectra obtained using a laser of 785 nm on DeltaNu Advantage Systems equipment.

The Raman spectrum for M0 micro wells corresponds to bands of calcite crystal standard described by Wehrmeister *et al.*³² with characteristic peaks observed at 154, 275, 712, 1085 and 1435 cm⁻¹, while the Raman spectrum for M10 micro wells is characteristic of vaterite.²⁵ In M1

to M6 micro wells both calcite and vaterite were present, and in M7 to M12 micro wells only vaterite was detected.

SEM of M0 micro wells showed a massive precipitation of rhombohedral crystals of calcite 20 to 25 μm in size and exhibiting regular $\{104\}$ faces (Fig. 3).

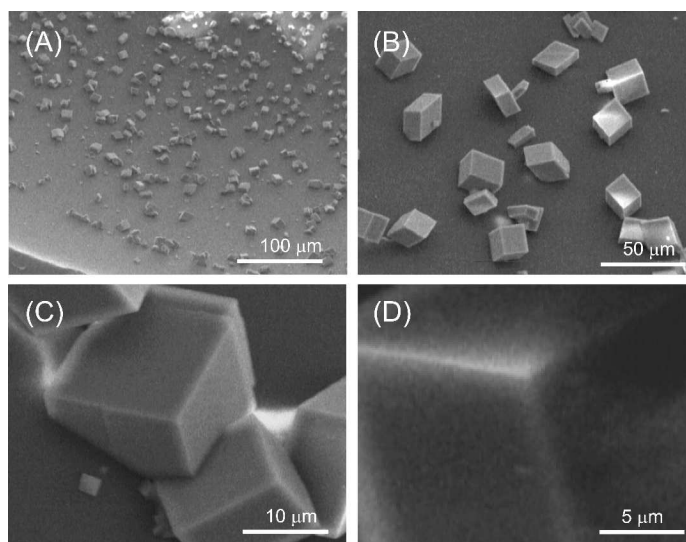


Fig. 3. SEM images of calcite crystals in the M0 micro well. In this micro well lecithin was not present.

The presence of lecithin has a strong effect on the morphology of the crystals formed. In M1 micro wells calcite crystals were obtained together with a few vaterite spherical particles. The shape of the calcite crystals appeared modified and showed cavities and curvatures (Fig. 4). In M2 and M3 micro wells the particles of calcite appeared to be formed by the assembly of rhombohedral units of micrometer and sub-micrometer sizes. This gave the final calcite particles a stepped and complex shape. These particles showed surfaces with cavities having micrometer

size curvatures (dotted curved lines in Fig. 4B) that formed sculpted architectures. Also, the vaterite particles changed their shape with respect to those in M1 micro wells, becoming less regular spherulites and having as building units irregular plate-like particles. In M4, M5 and M6 micro wells only a few aggregates of calcite (Fig. 5F) were observed, similar to those observed in M2 and M3 micro wells, and big spherulitic vaterite crystals were also observed. The spherulitic crystals of vaterite changed their texture quite drastically from M4 to M6 micro wells. Indeed the plate-like crystals forming the spherulites almost disappeared and spheroidal grains appeared (Fig. 5C, E, I).

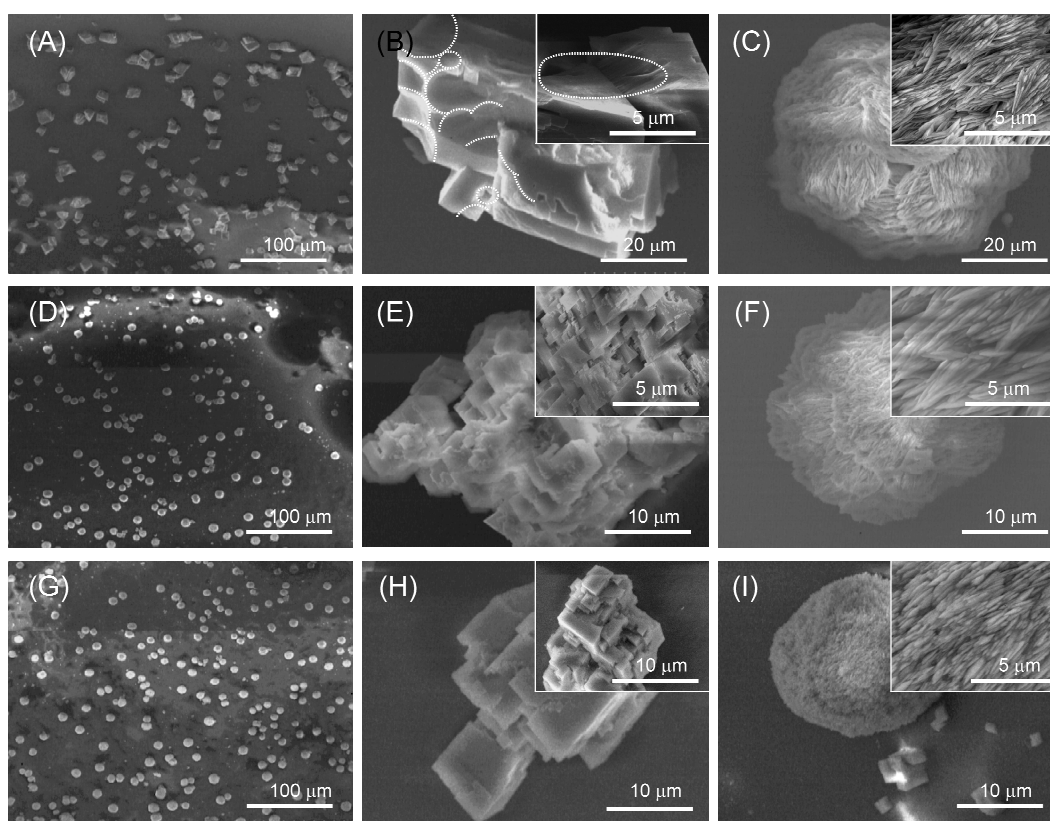


Fig. 4. SEM images of CaCO₃ particles precipitated in M1 (A-C), M2 (D-F) and M3 (G-I) micro wells. The morphology and shape of these particles are representative of the entire sample population, while their size can be diverse from the average. The dotted lines in (B) demarcate the borders of some of the cavities on the surface of the crystals.

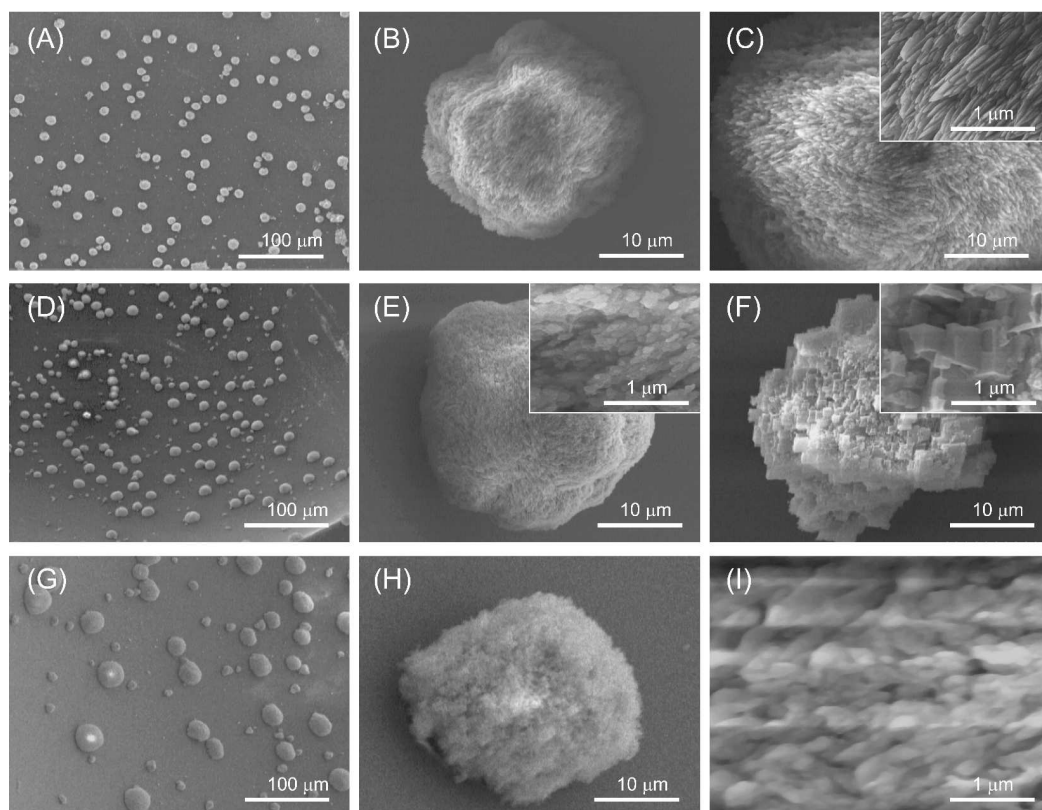


Fig. 5. SEM images of CaCO_3 particles precipitated in M4 (A-C), M5 (D-F) and M6 (G-I) micro wells. In B, C, E, H and I vaterite crystals are shown. In F an aggregate of calcite is shown. The morphology and shape of these particles are representative of the entire sample population, while their size can be diverse from the average.

In M7 to M12 micro wells only vaterite was detected (Figs 6 and 7). The particles appeared as irregular spheres formed by the assembly of nanoparticles that changed structure from one micro well to another. In M7 (Fig. 6) and M10 (Fig. 7) quite regular rhombohedral grains were observed with a size around 100 nm (Fig. 7C). In M8 (Fig. 6) and M11 micro wells (Fig. 7) the presence of vaterite formed by irregularly aggregated leaf-like layers a few nanometers in thickness was observed. In M9 and M12 micro wells (Figs 6 and 7) the presence of almost shapeless particles was observed. These particles locally appeared as compact materials in which randomly distributed pores were present (black regions in the SEM pictures in Figs 6I and 7I).

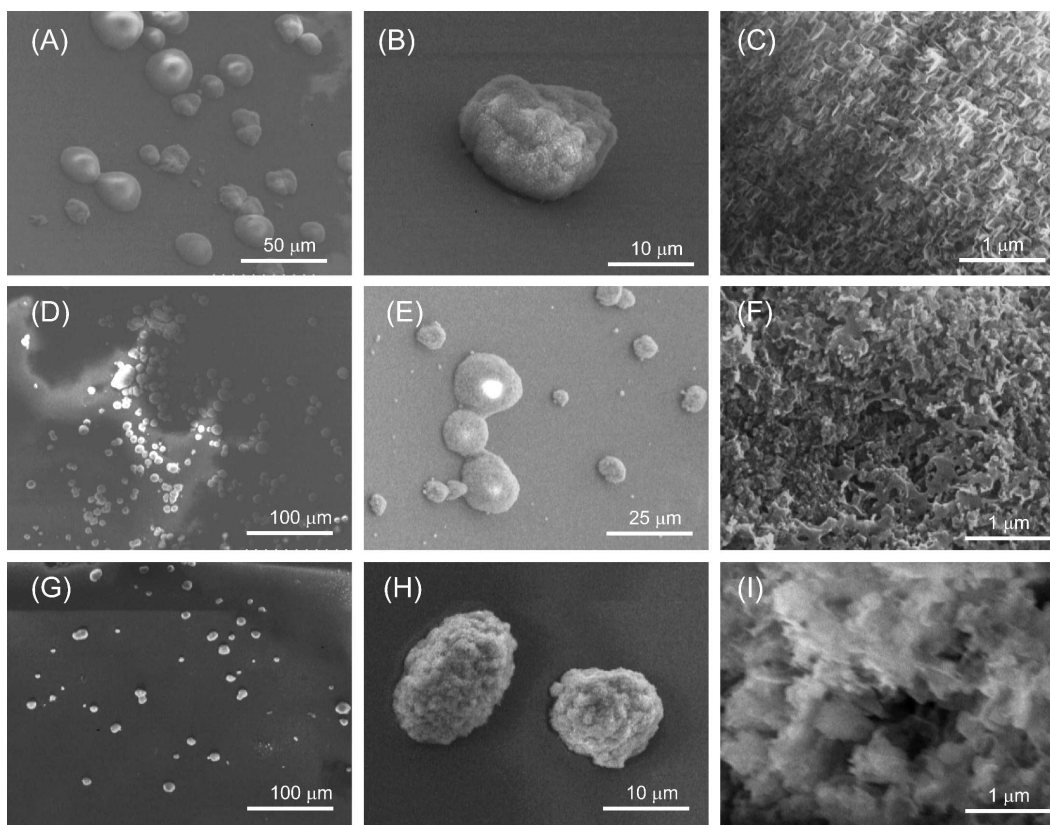


Fig. 6. SEM images of CaCO_3 particles precipitated in M7 (A-C), M8 (D-F) and M9 (G-I) micro wells. The morphology and shape of these particles are representative of the entire sample population, while their size can be diverse from the average.

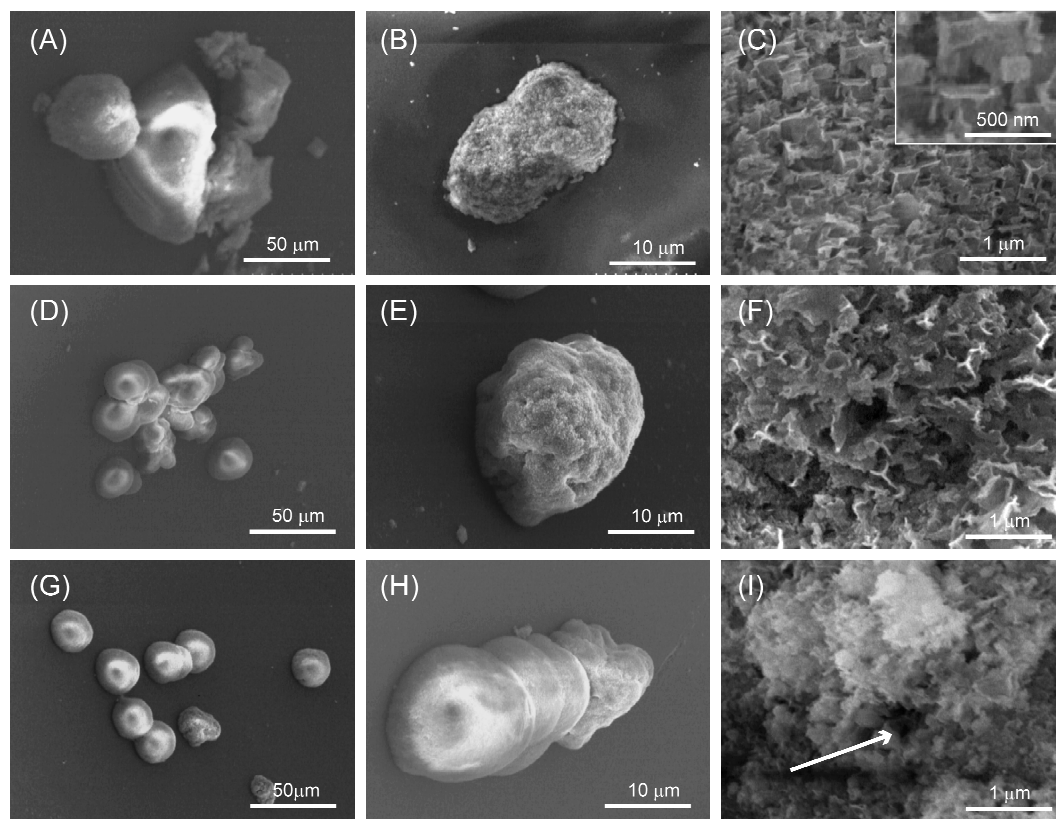


Fig. 7. SEM images of CaCO_3 particles precipitated in M10 (A-C), M11 (D-F) and M12 (G-I) micro wells. The arrow indicates a hole observed in the particle. The morphology and shape of these particles are representative of the entire sample population, while their size can be diverse from the average.

The distribution of CaCO_3 polymorph type and size varied for the crystals according to lecithin concentration (Fig. 8).

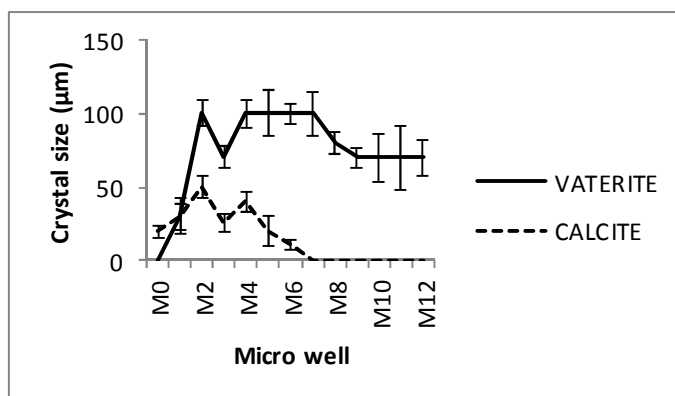


Fig. 8. The graph shows the type and size of crystals obtained in each micro well as a function of lecithin concentration (mean \pm SD).

Variability in the size of calcite crystals was observed among different types of micro wells. However, in each particular micro well, calcite crystal size was fairly uniform except when 17.5 μ l of lecithin was used (M5 micro well), where a much greater size distribution was observed (Table 2).

Table 2. Morphological features and size of calcite and vaterite crystals obtained in each micro well (mean \pm S.D.).

MICRO WELL CODE	CALCITE SHAPE / TEXTURE	CALCITE SIZE (μ m)	VATERITE SIZE (μ m)	CALCITE SHAPE / TEXTURE
M0	rhomb. {10.4} / single crystals	20.00 \pm 4.08	-	
M1	modified rhomb./ {10.4} single crystals	29.00 \pm 8.87	32.75 \pm 12.62	spherulites /plate-like crystals
M2	rhomb. {10.4} faced / polycryst. assemblies	50.00 \pm 7.43	100.25 \pm 8.96	spherulites /plate-like crystals
M3	rhomb. {10.4} faced / polycryst. assemblies	24.50 \pm 6.04	71.25 \pm 7.41	spherulites /plate-like crystals

M4	rhomb. {10.4}faced / polycryst. assemblies	39.50 ± 7.12	100.75±9.36	spherulites /plate- like crystals
M5	rhomb. {10.4}faced / polycryst. assemblies	20.75 ± 10.31	100.00±15.73	spherulites /spheroidal grains
M6	rhomb. {10.4}faced / polycryst. assemblies	10.15 ± 3.47	100.50±6.73	spherulites /spheroidal grains
M7		-	99.5±15.04	spherulites /compact spheroidal grains
M8		-	79.00±7.71	spherulites /compact spheroidal grains
M9		-	70.00±7.75	spherulites /pored spheroidal grains
M10		-	70.00 ±15.98	spherulites /compact spheroidal grains
M11		-	70.00 ±22	spherulites /thin platelike crystals
M12		-	61.50±15.31	spherulites /shapeless grains

Except for M1 micro wells, vaterite particles (73.66±31.39 μm) were always bigger than calcite crystals (14.95±17.22 μm). At intermediate concentrations the crystals were more homogeneous in size than in extreme concentrations, especially for crystals obtained with the 300 mg/ml lecithin solution. Calcite crystals are formed only below 35μg of lecithin in 35 μL of buffered CaCl₂ solution. In higher concentrations of lecithin only vaterite was formed. When Table 1 and 2 are compared it was observed that calcite crystal size decreased with the increase of lecithin concentration.

Discussion

Different CaCO₃ polymorphs (calcite, aragonite and vaterite) can be formed depending on the conditions of crystallization. Calcite is the most thermodynamically stable polymorph, but vaterite and aragonite can form under specific kinetic conditions and be precursors of calcite. Other studies of CaCO₃ nucleation and the influence of proteins on CaCO₃ formation involved

formation of CaCO_3 by vapor diffusion with set-ups similar to that used in the present study.^{35,36} In these studies it was shown that not only the concentration and nature of the additive influence nucleation and the specific polymorph(s) formed, but also the way in which the experimental system becomes supersaturated influences such variables.^{35,36} In fact, Gomez-Morales et al.³⁶ have shown that under the conditions of their experimental set-up, calcite, aragonite and vaterite precipitated in the absence of any additive. However, with the same chamber we have demonstrated that, using buffered solutions, it is possible to select only calcite or a mixture of two or three polymorphs, depending on the diameter of the central hole (controlled gas diffusion) or by altering the time of incubation or the incubation temperature.³⁷

The analysis of the distribution of polymorph gives information on the mechanism of precipitation. Raman spectroscopy is an appropriate method for monitoring the formation and evolution of CaCO_3 polymorphs.³⁸ These analyses showed the presence of calcite and vaterite in the micro wells when lecithin was used as additive.

The results of dynamic light scattering analysis show that lecithin assembly is not strongly affected by its concentration until a highly viscous sol forms (Table 1). Different crystal morphologies were obtained when lecithin concentration was increased, confirming the strong interaction of the CaCO_3 crystals with the lecithin molecular assemblies. In fact, it has been proposed that calcite crystal growth is guided by lipid templates, described as an intermicellar growth,²⁴ where the surface of the micelles or liposomes has a strong interaction with calcium ions causing crystallization between the micelles. Indeed, divalent cations have strong propensity to bind with the phosphocholine headgroups of lecithin³⁹ and tend to form more stable micelles.⁴⁰ In addition, it is also known that salts reduce the critical micelle concentration and that they can induce a transition from spherical to long cylindrical micelles (also called wormlike

micelles or worms), reducing the electrostatic repulsions between the charged surfactant headgroups (in effect decreasing the Debye screening length), which facilitates micellization and assembly into cylindrical structures.⁴¹ This can be observed in crystals obtained in the presence of a small amount of lecithin (until 5.6 μg , M3 micro well), where calcite crystals of uniform size, but with different degrees of surface modification were observed. Interestingly, at this small concentration of the lipid we also observed some vaterite crystals.

The characteristics of micelles are dependent on the emulsion in which they are formed. There are different types of emulsions, such as oil in water emulsions, wherein traditional micelles are formed with polar heads outward and hydrophobic tails toward the inside. However, in water in oil emulsions reversed micelles can also be formed in which the polar heads of the micelles are arranged inward and the hydrophobic tails outwards. Such micelles are formed to achieve a thermodynamic equilibrium, and it has been found that reversed micelles constitute stable compartments that serve as crystallization templates.⁴² In addition, in a CaCO_3 crystallization study conducted by Kang *et al.*⁴³, calcite crystals were obtained when low amounts of micelles were formed. However, by increasing the amount of surfactants, reversed micelles were formed and vaterite crystals were obtained. Normally lecithin reversed spherical or ellipsoidal micelles are obtained when additional surfactant, nonpolar organic solvents or oils are added^{44,45}, in the absence of bivalent ions or buffered solutions. However, it has been shown that inorganic salts can modulate the self-assembly of phospholipids like lecithin in organic solvents by binding with the phosphocholine headgroups of lecithin and induce a transition from spherical reversed micelles to cylindrical fibrils.⁴⁶ However, it is important to keep in mind that lecithin is a zwitterionic surfactant that in our experimental conditions (i.e., in the presence of 200 mM CaCl_2 in a pH 9 TRIS buffer solution) has highly ionized negatively charged phosphate groups in the

polar region of the molecule where a strong interaction with calcium ions is expected to occur. In fact, such calcium concentration-dependent interaction has been recently reported.³⁹ In addition, it has been reported previously that the binding of Ca^{2+} and other multivalent metal ions causes a small conformational change of the phosphocholine polar group.^{47,48} Moreover, in the case of bilayered phosphocholine, the binding of Ca^{2+} appears to involve the formation of a well-defined chemical complex in which one Ca^{2+} coordinates with two phosphocholine molecules.⁴⁹

In the present study, we showed that by increasing lecithin concentration in TRIS-buffered CaCl_2 solution, a change from hydrophilic to hydrophobic environment occurs, in which conductivity is drastically reduced, determining not only the type of CaCO_3 polymorph obtained, but also where the crystal is formed. In very dilute lecithin solutions (0.56 μg) vaterite formation occurred, although calcite was predominant. This could reflect the ability of lecithin molecules to nucleate and stabilize vaterite crystals, which are inherently unstable in aqueous solution. The presence of some worm-like aggregates of two to eight vaterite crystals reported herein correlates with a statement by Eastoe *et al.*⁴² that the reversed micelles, formed in the presence of additional surfactants, restrict random movements, which can facilitate contact between two or more micelles. The more hydrophobic environment obtained under these conditions as a function of the amount of lecithin, should correspond to the formation of a complex highly viscous sol network. Therefore, this indicates that the vaterite crystals reported herein were formed inside ionized aqueous confined spaces which are specified by the geometry of the micelles and which lie between the hydrophilic oily tails of the lecithin molecules, while the calcite crystals with surface modification preferentially form in the intermicellar spaces of regular micelles. This is consistent with our observation that calcite disappeared and vaterite became the only polymorph when lecithin concentration was increased. The diverse textures of the vaterite crystals obtained

in this study (i.e., grains, leaf-like layers) is an indication that higher lecithin concentrations produce an environment consisting of a complex network, which contains confined aqueous charged spaces that act as templates for crystallization of vaterite and in which the occurrence of reversed micelles cannot be disregarded. This could be related to the observation reported by Kang *et al.*⁴³, that similar vaterite crystals were favored when the surfactant content (sodium dodecyl sulfate) was increased in the reversed micelles. These authors demonstrated that there is an effective supersaturation induced in the micelles, which is much higher than that in the bulk aqueous solution. In fact, it has recently been demonstrated that under high supersaturation the growth of pumpkin-shaped vaterite, such as that reported here, is favored.¹⁴ Occurrence of vaterite has been reported in reversed micelles of cetyl trimethylammonium bromide surfactant at 5 °C.⁵⁰ Under our experimental conditions, the formation of vaterite when lecithin concentration was increased requires conditions of high supersaturation. The aspect ratio of the confined continuous or discontinuous aqueous spaces containing 200 mM CaCl₂ in pH 9 TRIS buffer solution, present in the viscous sol at high lecithin concentrations, determines the conditions of the required supersaturation. This is because there is an increase in the water that is bound to the charged surface and is also due to a preferential solubility and diffusivity of the lipophilic CO₂ through the lipid matrix, as has been demonstrated elsewhere.^{51, 52}

The morphology of the crystals changes with lecithin concentration and also with the procedure for preparing the lecithin media. Indeed, morphological differences were observed between crystals that were obtained from different lecithin media with the same final lecithin concentration. An example is given by the crystals obtained in M9 and M11 micro wells, which both have a final lecithin concentration of 525 µg. However, the M9 micro well was prepared using the stock solution of 150 mg/ml and the M11 micro well was prepared with the stock

solution of 300 mg/ml. This indicates that the geometry or spatial distribution of the continuous or discontinuous ionic confined aqueous spaces in the viscous sol is already determined at an early stage of lecithin molecule assembly.

Controlling polymorphism has great technological significance especially because it can determine specific mechanical or optical properties of materials. In addition polymorphism is important in many fields like pharmaceuticals, agrochemicals, pigments and foods where dissolution rates depend on polymorphism. Here, we demonstrated that it is possible to get different proportions of calcium carbonate polymorphs depending on the lecithin concentration in the crystallization medium.

Conclusions

In summary, herein we demonstrated that the occurrence of both surface-modified calcite crystals and diverse textured vaterite crystals that are formed in an ionized calcium chloride solution under a continuous CO₂ diffusion atmosphere reflects the geometry and spatial distribution of ionized aqueous confined spaces due to the specifics of lecithin assembly, which are largely controlled by lecithin concentration. The results obtained, in conjunction with the related discussion, suggest that as a function of lectin concentration the precipitation of CaCO₃ occurs inter-micelle, producing sculpted crystals of calcite, or intra-reversed micelle, producing different assemblies of vaterite crystals. To demonstrate these precipitation paths, which has implications for biomineralization as well as in material science, further studies will be needed to determine the exact type and characteristics of the arrangement of lecithin molecules (i.e., micelles, reversed micelles, layers, worm-like tubes, etc.) in each lecithin medium. However, the presence of different polymorphs and surface modifications observed in this study is compatible with the occurrence and effect of traditional and reversed micelles determining special

confinement spaces where crystallization of CaCO₃ occurs in the different lecithin concentration media.

Acknowledgements

This work was supported by FONDECYT 1120172, granted by the Chilean Council for Science and Technology (CONICYT) and Project N° 5788 04/02/2013, Agreement University of Bologna-University of Chile. Authors thank Dr. David Carrino from Case Western Reserve University for grammatical revision of the manuscript.

Notes and references

- 1 L. H. Lowenstam and S. Weiner, *On Biomineralization*, 1989.
- 2 A. H. Heuer, D. J. Fink, V. J. Laraia, J. L. Arias, P. D. Calvert, K. Kendall, G. L. Messing, P. C. Rieke, D. H. Thompson, A. P. Wheeler, A. Veis and A. I. Caplan, *Science*, 1992, **255**, 1098-1105.
- 3 G. Falini and S. Fermani, *Cryst. Res. Technol.*, 2013, **48**, 864-876.
- 4 L. Addadi and S. Weiner, *Proc. Natl. Acad. Sci. U. S. A.*, 1985, **82**, 4110-4114.
- 5 A. M. Belcher, X. H. Wu, R. J. Christensen, P. K. Hasma, G. D. Stucky and D. E. Morse, *Nature*, 1996, **381**, 56-58.
- 6 G. Falini, S. Albeck, S. Weiner and L. Addadi, *Science*, 1996, **271**, 67-69.
- 7 J. L. Arias and M. S. Fernandez, *Chem. Rev.*, 2008, **108**, 4475-4482.
- 8 F. C. Meldrum and H. Cölfen, *Chem. Rev.*, 2008, **108**, 4332-4432.
- 9 X. H. Guo, S. H. Yu and G. B. Cai, *Angew. Chem. Int. Ed.*, 2006, **45**, 3977-3981.
- 10 X. H. Guo, F. Meng, X. Qu, M. Wang, C. Mao, J. Zhang, W. Wang and S. H. Yu, *CrystEngComm*, 2012, **14**, 3213-3219.
- 11 S. Hutchens, R. Benson, B. Evans, H. O'Neill and C. Rawn, *Biomaterials*, 2006, **26**, 4661-4670.
- 12 L. M. Hamm, A. J. Giuffre, N. Han, J. Tao, D. Wang, J. J. De Yoreo and P. M. Dove, *Proc. Natl. Acad. Sci., U. S. A.* 2014, **111**, 1304-1309.

- 13 E. Loste, R. Wilson, R. Seshadri and F. C. Meldrum, *J. Cryst. Growth*, 2003, **254**, 206-218.
- 14 Y. Xu, G. Ma and M. Wang, *Cryst. Growth Des.*, 2014, **14**, 6166-6177.
- 15 L. Gower, *Chem. Rev.*, 2008, **108**, 4551-4627.
- 16 E. Loste, R. J. Park, J. Warren and F. C. Meldrum, *Adv. Funct. Mater.*, 2004, **14**, 1211-1220.
- 17 C. J. Stephens, S. F. Ladden, F. C. Meldrum and H. K. Christenson, *Adv. Funct. Mater.*, 2010, **20**, 2108-2115.
- 18 C. J. Stephens, Y. Y. Kim, S. D. Evans, F. C. Meldrum and H. K. Christenson, *J. Am. Chem. Soc.*, 2011, **133**, 5210-5213.
- 19 M. Kellermeier, E. Melero-Garcia, F. Glaab, R. Klein, M. Drechsler, R. Rachel, J. M. Garcia-Ruiz and W. Kunz, *J. Am. Chem. Soc.*, 2010, **132**, 17859-17866.
- 20 (a) C. C. Tester, R. E. Brock, C.-H. Wu, M. R. Krejci, S. Weigand and D. Joester, *CrystEngComm*, 2011, **13**, 3975-3978; (b) C. C. Tester, C. H. Wu, S. Weigand and D. Joester, *Faraday Discuss.*, 2012, **159**, 345-356.
- 21 I. Rodríguez-Ruiz, S. Veessler, J. Gómez-Morales, J. M. Delgado-López, O. Grauby, Z. Hammadi, N. Candoni, and J. M. García-Ruiz, *Cryst. Growth Des.*, 2014, **14**, 792-802.
- 22 M. Prieto, *Mineralogical Magazine*, 2014, **78**, 1437-1447.
- 23 J. L. Arias and M. S. Fernandez, *Mater. Charact.*, 2003, **50**, 189-195.
- 24 P. Wan, Y. Zhao, H. Tong, Z. Yang, Z. Zhu, X. Shen and J. Hu, *Mater Sci Eng C*, 2009, **29**, 222-227.
- 25 A. Szczes, *Colloids Surf B*, 2013, **101**, 44-48.
- 26 T. Lee and J. G. Chen, *Cryst. Growth Des.*, 2009, **9**, 3737-3748.
- 27 S. Mann, J. P. Hannington and R. J. P. Williams, *Nature*, 1986, **324**, 565-567.
- 28 G. A. Ozin, *Acc. Chem Res.*, 1997, **30**, 17-27.
- 29 P. Pal, T. Kamilya, S. Acharya and G. B. Talapatra, *J. Phys. Chem. C*, 2010, **114**, 8348-8352.
- 30 A. L. Litvin, L. A. Samuelson, D. H. Charych, W. Spevak and D. L. Kaplan, *J. Phys. Chem.*, 1995, **99**, 12065-12068.
- 31 K. Gopal, Z. Lu, M. M. de Villiers and Y. Lvov, *J. Phys. Chem. B*, 2006, **110**, 2471-2494.
- 32 J. M. Dominguez-Vera, J. Gautron, J. M. Garcia-Ruiz, Y. Nys, *Poultry Sci.*, 2000, **79**, 901-907.
- 33 C. Jimenez-Lopez, A. Rodriguez-Navarro, J. M. Dominguez-Vera and J. M. Garcia-Ruiz,

- Geochim. Cosmochim. Acta*, 2003, **67**, 1667-1676.
- 34 U. Wehrmeister, A. L. Soldati, D. E. Jacob, T. Häger and W. Hofmeister, *J. Raman Spectrosc.*, 2010, **41**, 193-201.
- 35 A. Hernández-Hernández, A. B. Rodríguez-Navarro, J. Gómez-Morales, C. Jiménez-Lopez, Y. Nys and J. M. García-Ruiz, *Cryst. Growth Des.*, 2008, **8**, 1495–1502.
- 36 J. Gomez-Morales, A. Hernandez-Hernandez, G. Sazaki, and J. M. García-Ruiz *Cryst. Growth Des.*, 2010, **10**, 963-969.
- 37 A. C. Neira, M. S. Fernandez, J. Retuert and J. L. Arias, *Mat. Res. Soc. Symp. Proc.*, 2004, **EXS-1**, 321-326.
- 38 P. Agarwal and K. Berglund, *Cryst. Growth Des.*, 2003, **3**, 941-946.
- 39 P. B. Santhosh, S. I. Kiryakova, J. L. Genova and N. P. Ulrich, *Colloids Surf. A*, 2014, **460**, 248-253.
- 40 Y. X. Huang, R. C. Tan, Y. L. Li, Y. Q. Yang, L. Yu and Q. C. He, *J. Colloid Interf, Sci.*, 2001, **236**, 28-34.
- 41 C. A. Dreiss, *Soft Matter*, 2007, **3**, 956-970.
- 42 J. Eastoe, M. Hollamby and L. Hudson, *Adv. Colloid Interface Sci.*, 2006, **128**, 5-15.
- 43 S. H. Kang, I. Hirasawa, W. S. Kim, and C. K. Choi, *J. Colloid. Interf. Sci.*, 2005, **288**, 496-502.
- 44 D. M. Willard, R. E. Riter, and N. E. Levinger, *J. Am. Chem. Soc.*, 1998, **120**, 4151-4160.
- 45 Y. A. Shchipunov, *Colloid Surf. A*, 2001, **183**, 541-554.
- 46 H. Y. Lee, K. K. Diehn, S. W. Ko, S. H. Tung and S. R. Raghavan, *Langmuir*, 2010, **26**, 13831-13838.
- 47 M. F. Brown and J. Seelig, *J. Biochem.*, 1978, **17**, 381-384.
- 48 H. Akutsu and J. Seelig, *J. Biochem.*, 1981, **20**, 7366-7373.
- 49 C. Altenbach and J. Seelig, *J. Biochem.*, 1984, **23**, 3913-3920.
- 50 A. Ganguli, J. Ahmed, S. Viadya and T. Ahmad, *J. Nanosci. Nanotechnol.*, 2007, **7**, 1760-1767.
- 51 A. Hulikova and P. Swietach, *FASEB J.*, 2014, **28**, 2762-2774.
- 52 A. Missner, P. Kügler, S. M. Saparov, K. Sommer, J. C. Mathai, M. L. Zeidel, and P. Pohl, *J. Biol. Chem.*, 2008, **283**, 25340-28347.

TABLE OF CONTENTS

This research shows that by tailoring the assembly of lecithin molecules it is possible to modulate texture, polymorphism, size and shape of calcium carbonate crystals. The occurrence of surface-modified calcite crystals and diverse textured vaterite crystals in an ionized calcium chloride solution under a continuous CO₂ diffusion atmosphere was shown to reflect the geometry and spatial distribution of aqueous confined spaces due to the lecithin assembly that is largely controlled by lecithin concentration.

